

Article

# Physicochemical Model of Formation of Gold-Bearing Magnetite-Chlorite-Carbonate Rocks at the Karabash Ultramafic Massif (Southern Urals, Russia)

Valery Murzin <sup>1</sup> , Konstantin Chudnenko <sup>2</sup>, Galina Palyanova <sup>3,4,\*</sup>, Aleksandr Kissin <sup>1</sup> and Dmitry Varlamov <sup>5</sup> 

<sup>1</sup> A.N. Zavaritsky Institute of Geology and Geochemistry, Ural Branch of Russian Academy of Sciences, Vonsovskogo str., 15, Ekaterinburg 620016, Russia; murzin@igg.uran.ru (V.M.); kissin@igg.uran.ru (A.K.)

<sup>2</sup> A.P. Vinogradov Institute of Geochemistry, Siberian Branch of Russian Academy of Sciences, Favorskogo str., 1a, Irkutsk 664033, Russia; chud@igc.irk.ru

<sup>3</sup> V.S. Sobolev Institute of Geology and Mineralogy, Siberian Branch of Russian Academy of Sciences, Akademika Koptyuga pr., 3, Novosibirsk 630090, Russia

<sup>4</sup> Department of Geology and Geophysics, Novosibirsk State University, Pirogova str., 2, Novosibirsk 630090, Russia

<sup>5</sup> Institute of Experimental Mineralogy, Russian Academy of Sciences, Chernogolovka, Moscow Region 142432, Russia; dima@iem.ac.ru

\* Correspondence: palyan@igm.nsc.ru

Received: 8 June 2018; Accepted: 17 July 2018; Published: 20 July 2018



**Abstract:** We present a physicochemical model for the formation of magnetite-chlorite-carbonate rocks with copper gold in the Karabash ultramafic massif in the Southern Urals, Russia. The model was constructed based on the formation geotectonics of the Karabash massif, features of spatial distribution of metasomatically altered rocks in their central part, geochemical characteristics and mineral composition of altered ultramafic rocks, data on the pressure and temperature conditions of formation, and composition of the ore-forming fluids. Magnetite-chlorite-carbonate rocks were formed by the hydrothermal filling of the free space, whereas chloritoidites were formed by the metasomatism of the serpentinites. As the source of the petrogenic and ore components, we considered rocks (serpentinites, gabbro, and limestones), deep magmatogenic fluids, probably mixed with metamorphogenic fluids released during dehydration and deserpentinization of rocks in the lower crust, and meteoric waters. The model supports the involvement of sodium chloride-carbon dioxide fluids extracting ore components (Au, Ag, and Cu) from deep-seated rocks and characterized by the ratio of ore elements corresponding to Clarke values in ultramafic rocks. The model calculations show that copper gold can also be deposited during serpentinization of deep-seated olivine-rich rocks and ore fluids raised by the tectonic flow to a higher hypsometric level. The results of our research allow predicting copper gold-rich ore occurrences in ultramafic massifs.

**Keywords:** Karabash ultramafic massif; magnetite-chlorite-carbonate rocks; chloritoidites; Au-Cu mineralization; copper gold; thermodynamic modeling

## 1. Introduction

The Karabash ophiolite massif is located within a belt of ultramafic massifs stretching along the Main Ural fault zone in the Southern Urals (Figure 1) [1,2]. The massif became widely known after the discovery of the gold-copper (Au-Cu) mineralization at the Zolotaya Gora gold deposit. The main ore bodies at this deposit are represented by rodingites (“chlogropites”), which consist of chlorite, garnet, pyroxene and a minor quantity of calcite. These rocks contain a specific Au-Cu

mineralization: tetra-auricupride ( $\text{AuCu}$ ), auricupride ( $\text{AuCu}_3$ ),  $\text{Au}_3\text{Cu}$ , and solid solutions of the gold-silver-mercury ( $\text{Au-Ag-Hg}$ ) system [3–6]. The other gold occurrence at the Karabash massif was recognized in the magnetite-chlorite-carbonate rocks that are accompanied by strongly chloritized serpentinites (chloritolites) [7,8], where native gold is characterized by high fineness and Cu content of 1.3–2.6 wt %. These types of rocks are also known for their increased Y, Zr, REE, U and Th contents.

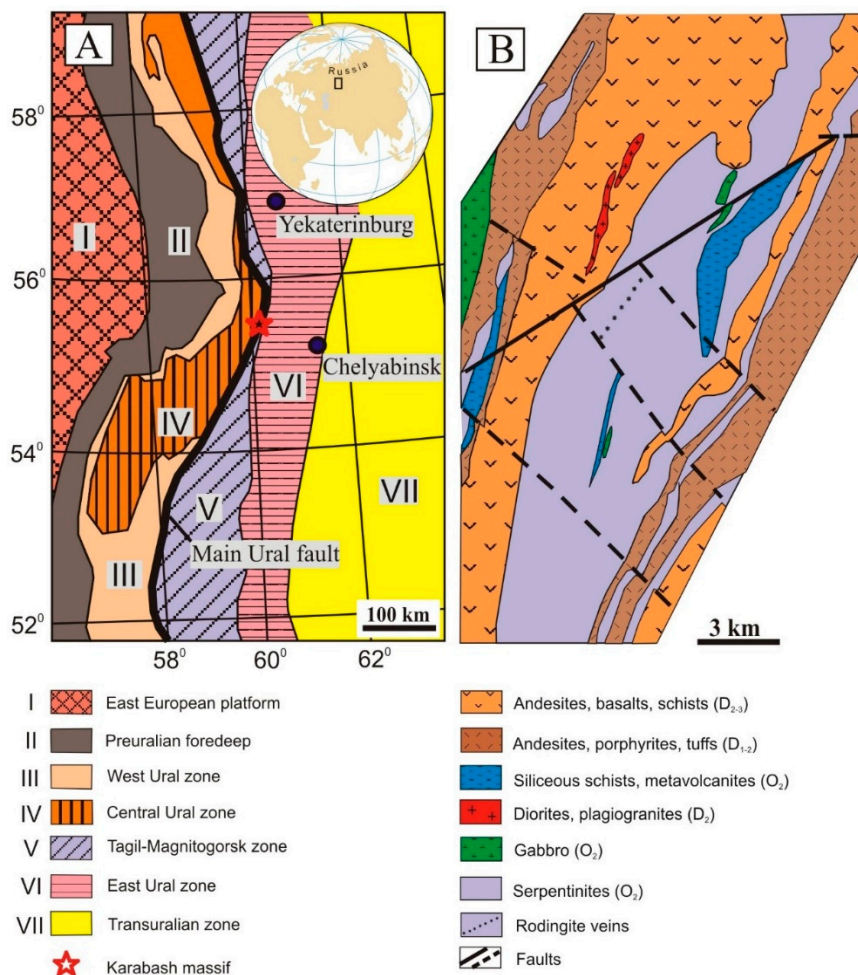


**Figure 1.** Karabash ultramafic massif (Southern Urals, Russia). (A) Position of the Karabash massif on the tectonic scheme of Urals per Puchkov [1]. (B) Schematic geological map of the Karabash massif (modified from Snachyov et al. [2] with authors' additions).

Earlier mineralogical-geochemical and isotope studies of magnetite-chlorite-carbonate and strongly chloritized rocks (chloritolites) [8,9] provide an opportunity for the reconstruction of a physicochemical model of the formation of these rocks and the deposition of copper gold within. Construction of this model was the main goal of our study. The model was calculated considering that: (1) the formation of magnetite-chlorite-carbonate rocks involves the participation of hydrothermal solution by the mechanism of free space filling, and chloritolites are formed by the mechanism of replacement of the serpentinite rocks; and (2) the most likely sources for petrogenic and ore components are: (a) rocks (serpentinite, gabbro, and limestone), (b) deep magmatogenic fluid, probably mixed with the metamorphogenic fluid released during dehydration and deserpentinization of the lower crustal rocks, and meteoric water.

## 2. Geological Background of the Studied Area

### 2.1. Geological Setting of the Karabash Massif and Hydrothermal-Metasomatic Rocks

The Karabash ultramafic massif is composed of antigorite and, to a lesser extent, chrysotile and lizardite serpentinites. Various types of hydrothermal-metasomatic rocks in the massif are spatially separated but have similar geologic settings, being localized in zones of tectonic mélangé or at the contacts of the massif (Figure 2a) [10]. The belt of rodingite rocks extends continuously for about 2.5 km along the central part of the massif. The magnetite-chlorite-carbonate and riebeckite rocks occur locally only in its marginal parts. Listvenites are scarce; with a band up to 15 m thick with a diorite-porphyrite dike occurs in the western contact of the host volcano-sedimentary strata.

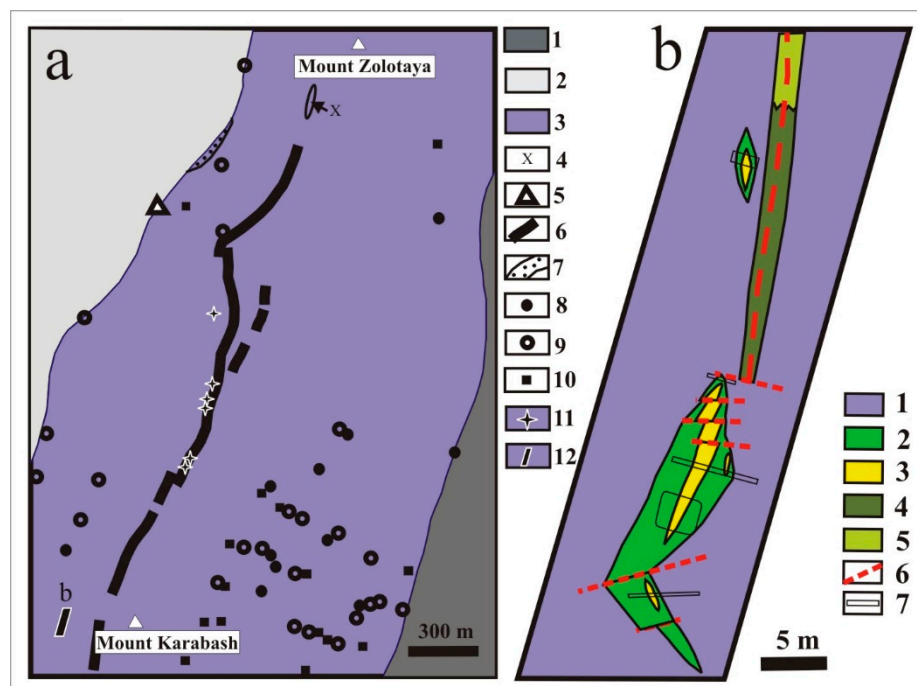


**Figure 2.** Geological position and types of hydrothermal-metasomatic rocks in the Karabash massif: (a) Spatial location of metasomatized rocks in the central part of the Karabash massif based on the geological map on a scale of 1:10,000 compiled by Lozhechkin [10] from the results of geological studies in 1933–1935. 1, Ordovician rocks of the Polyakovka Formation; 2, Devonian rocks of the Karamalytash and Ulutau Formations; 3, serpentinites; 4, diorite-porphyrites; 5, quartz diorite-porphyrites; 6–10, altered rocks: 6, rodingites; 7, listvenites; 8, epidote-chlorite-garnet; 9, magnetite-chlorite-carbonate; and 10, quartz-riebeckite; 11, mine workings (mines and adits) at the Zolotaya Gora deposit; and 12, location of the studied area. (b) Occurrence of lenses of magnetite-chlorite-carbonate rocks in the zone of foliated serpentinites in the west of the Karabash massif. 1, antigorite serpentinite; 2, chloritolite; 3, lenses of magnetite-chlorite-carbonate rocks; 4, intensely carbonatized serpentinite; 5, serpentinite with dispersed carbonate mineralization; 6, faults; 7, mine workings. Figure 2 is the reproduction of Figures 2 and 3 published in Murzin et al. [8].

Magnetite-chlorite-carbonate rocks and chloritolites occur nearby the zones of foliated serpentinites (Figure 2a, symbol 9). These zones are several hundred meters long and up to tens of meters thick. The lenticular bodies of magnetite-chlorite-carbonate rocks vary in size from few centimeters to several meters. The largest body that became the object for our study is about 20 m long and 2 m thick and occurs on the western slopes of Mt. Karabash (Figure 2a,b). The body is broken up by a series of transverse faults, which reveal the displacement of its contacts up to 1 m.

Zonation is visible between the ore body of the host antigorite serpentinites and the body of magnetite-chlorite-carbonate rocks, with intermediate zones of carbonatized and chloritized antigorite serpentinites and chloritolites (Figure 3). Zones of chloritolites bordering the magnetite-chlorite-carbonate body are nonsymmetrical in thickness. In the eastern contact, the thickness of the body is about 1.5 m, whereas in the western part it is only a few tens of centimeters.

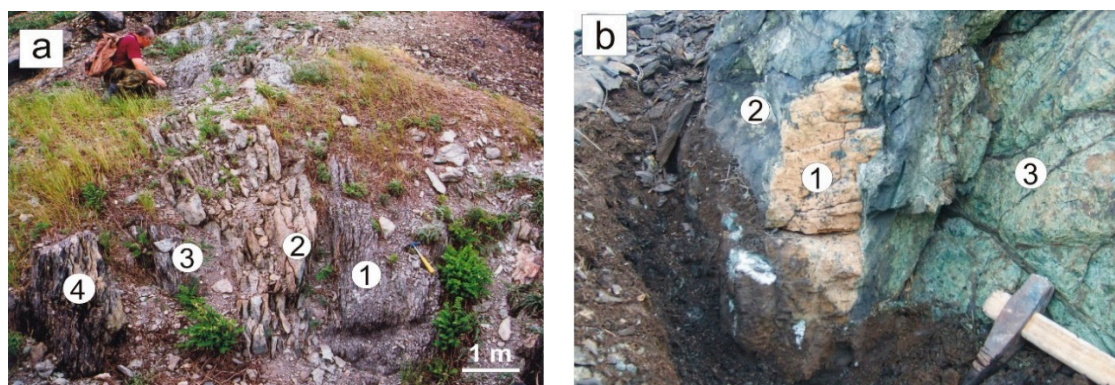


**Figure 3.** Zonation around (a) a large body and (b) a small lens of magnetite-chlorite-carbonate rocks. Zones: 1—magnetite-chlorite-dolomite, 2—chloritolite, 3—serpentinite with carbonatization and chloritization, 4—antigorite serpentinite. (a) The central zone (2) is composed of nearly equal amounts of carbonate and magnetite and a minor amount of chlorite, the content of which increases in the marginal parts of the zone. (b) The central zone (1) is composed of dolomite and a small amount of chlorite.

## 2.2. Mineral Composition of Altered Ultramafic Rocks

A detailed description of the mineral composition of magnetite-chlorite-carbonate rocks as well as hosting chloritolites and antigorite serpentinites was reported in our previous works [7,8]. Their description is outlined below.

Antigorite serpentinite consists of stellar and tabular aggregates of antigorite with rare grains of magnetite scattered within. The rock is rich in tiny magnetite, which is often concentrated into veins and chains confined to both antigorite and magnesite (Figure 4a). Scattered pentlandite and chromspinel are the accessory minerals of serpentinites. Here, newly formed dolomite and chlorite (clinocllore) are present, the content of which is as high as 30 vol %. Chromspinel is intensely replaced by chromium (Cr)-bearing clinocllore, chromian magnetite and magnetite.

Chloritolites, consisting of fine-grained colorless chlorite, contain scattered carbonate and thin veinlets of coarse-grained chlorite (Figure 4b). They also contain impregnations of magnetite and chromspinel, which definitively indicates the aposerpentinite nature of chloritolites. The composition of relict chromspinel was established to be similar to the accessory spinel from ophiolite harzburgites [7].

The magnetite-chlorite-carbonate rocks have various contents of minerals. Typically, the central parts of these rock bodies consist of carbonate mass (dolomite and, in smaller quantity, calcite), and the marginal parts are enriched in chlorite, magnetite, ilmenite, and apatite, the total content of which is 40–45 vol % (Figure 4c). As accessory minerals, the magnetite-chlorite-carbonate rocks also contain native gold, zircon, monazite, allanite, thorianite, aeschynite-(Y), and very scarce grains of chalcopyrite up to 2 mm in size. Relict chromspinel was absent in these rocks.

Native gold is represented by the particles of various interstitial shapes, up to 3 mm in size. The gold particles contain inclusions of magnetite, ilmenite, dolomite, apatite, and chlorite (Figure 4d). Gold belongs to the copper-bearing variety of gold-silver solid solutions (fineness 833–865‰). Impurity components of native gold (wt %) are as follows: Ag (10.8–13.5), Cu (1.3–2.6), Pd (0.06–0.95) and Fe (to 0.07) (Tescan VEGA-II XMU electron scanning microscope (TESCAN, Brno, Czech Republic))

with attached INCA Energy 450 energy-dispersive spectrometer (Oxford Instruments, Oxford, UK), analyst D. Varlamov, Institute of Experimental Mineralogy, Russian Academy of Sciences) [8].

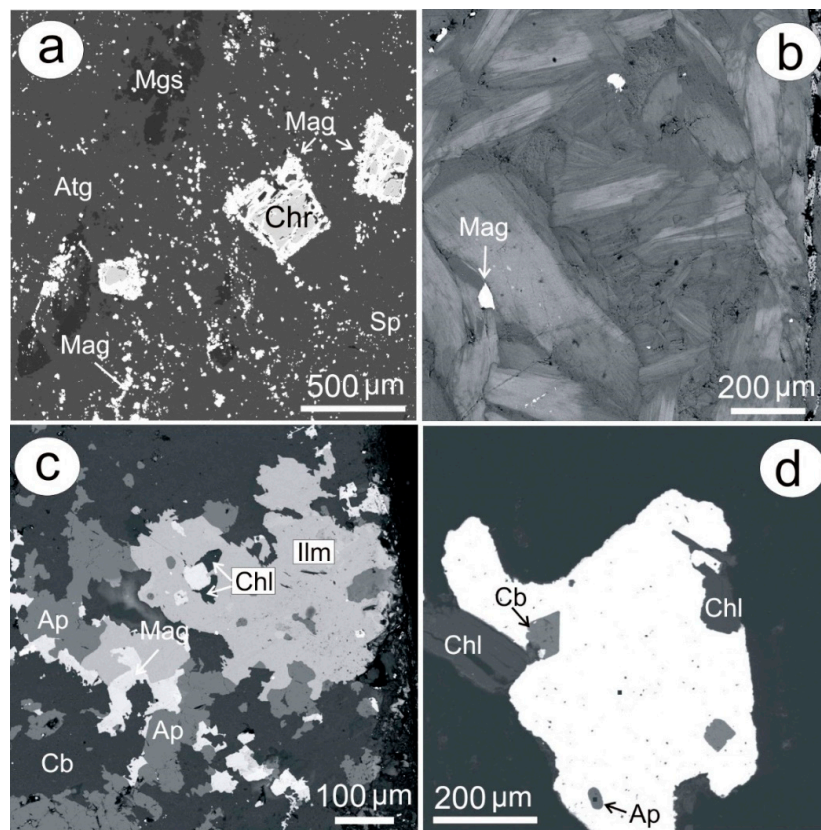


**Figure 4.** Relationships between minerals in altered ultramafic rocks from the Karabash massif. Back-scattered electron images of polished sections [8]: (a) Serpentinite including antigorite (Atg) with dispersed magnesite (Mgs), magnetite (Mag), and chromspinel (Chr). Chromspinel is replaced by magnetite. (b) Chloritolite composed of zoned chlorite grains with scarce impregnation of magnetite (Mag). Central parts of chlorite grains (light gray) contain 12–16 wt % FeO, marginal parts (dark gray), 5–7 wt % FeO. Magnetite-chlorite-carbonate rock: (c) intergrowths of apatite (Ap), ilmenite (Ilm), magnetite (Mag), chlorite (Chl), and carbonate (Cb); (d) copper gold with inclusions of chlorite (Chl), apatite (Ap), and carbonate (Cb).

No signs of multistage formation of magnetite-chlorite-carbonate rocks were clearly revealed. They only demonstrate post-ore tectonics. However, many minerals of these rocks, such as dolomite, chlorite, zircon, and aeschynite have two generations with distinct signs of the replacement of early generations by late ones.

### 2.3. Geochemical Characteristics of Rocks

The most complete data, including the distribution of rare earth elements (REE) in the rocks, reported in our previous work [8]. Here, we only outline the general regularities of trace elements in rock samples (Table S1). The sampling spots in the ditch are shown in Figure 3a. The trace element composition of rocks was determined by ICP MS on an ELAN 9000 Perkin Elmer mass spectrometer (PerkinElmer, Waltham, MA, USA, analyst D.V. Kiseleva, Institute of Geology and Geochemistry, Ural Branch of Russian Academy of Sciences).

Analysis of the trace element composition of rocks showed that antigorite serpentinite has increased contents of elements typical of ultramafic rocks: Cr, Ni, Co, as well as Mn and B. Some samples contained Cu, Zn, Hg, Cd, and Sb. In chloritolites and magnetite-chlorite-carbonate

rocks, the following elements are concentrated: Mn, Ba, Sr, Ti, V, Cu, As, Zr, Hf, Nb, Y, Mo, Ga, Ge, Sc, Ta, Li, Rb, Cs, U, Th, and REE. The total content of REE in serpentinites was less than 2 g/t, whereas in chloritolites and magnetite-chlorite-carbonate rocks it reached 304 g/t.

#### 2.4. *P,T-Conditions of Formation and Composition of Ore-Forming Fluid*

The temperature regime of the formation of magnetite-chlorite-carbonate rocks estimated using oxygen isotope and dolomite-calcite geothermometers [8] showed that these rocks formed at 480–280 °C. The homogenization temperature of gas-liquid (fluid) inclusions in apatite (THMSG-600 “Linkam” heating-freezing stage, Linkam Scientific, Tadworth, UK, analyst A.A. Garaeva, Institute of Geology and Geochemistry, Ural Branch of Russian Academy of Sciences), reflecting the minimal crystallization temperature of this mineral, was 142–221 °C [9]. The eutectic temperature varies from –19.0 to –23.0 °C, which corresponds to the H<sub>2</sub>O–NaCl system [11]. The melting temperature of ice ranges from –2.2 to –5.7 wt %, which corresponds to NaCl concentration in solution equal to 3.7–8.8 wt % [12].

The mineral formation derived temperature from the oxygen isotope and dolomite-calcite geothermometers exceeded the homogenization temperatures of fluid inclusions by 140–260 °C. Considering the pressure correction, which is 80–90 °C/kbar [13], the pressure during the formation of magnetite-chlorite-carbonate rocks could have reached 2–3 kbar.

The gas component content in fluid inclusions in the minerals of chloritolites and magnetite-chlorite-carbonate rocks [9], extracted by pyrolysis to 450 °C (below the decomposition temperature of carbonate), can be described using the C–H–O system with minor nitrogen. Composition of gases was analyzed on the Tsvet-800 gas chromatograph (SPE ACADEMPRYLAD Ltd., Sumy, Russia, analyst S.N. Shanina, Institute of Geology, Komi Science Centre, Ural Branch of Russian Academy of Sciences). The fluid was dominated by water and carbon dioxide and contained small amounts of reduced gases: CO, H<sub>2</sub>, CH<sub>4</sub>, and heavy hydrocarbons including C<sub>2</sub>H<sub>4</sub>, C<sub>2</sub>H<sub>6</sub>, C<sub>3</sub>H<sub>6</sub>, C<sub>3</sub>H<sub>8</sub>, etc. The degree of oxidation of the gas components (CO<sub>2</sub>/(CO<sub>2</sub> + CO + H<sub>2</sub> + CH<sub>4</sub>)) in the fluid for magnetite-chlorite-carbonate rock was higher than that of chloritolites, at 0.92 and 0.73, respectively.

#### 2.5. *Sources of Metals and Ore-Bearing Fluid*

High content of gold, Y, Zr, REE, U and Th, the absence of any essential input of K and Na, and rather low scales of mineralization allow us to regard the same rock reservoir as the source of these elements. Data on the isotope composition of C, O, and Sr in carbonates [8] show that in the generation of ore-forming fluids the marine carbonate reservoir was also involved. The restoration of the isotope composition of the water of these fluids suggests that they have been of metamorphogenic origin and have been composed of a mixture of at least two water sources—rock (dehydration of water derived from serpentinite) and deep-seated reservoirs. Taking into consideration that the isotope composition of serpentinite hydrogen, which typically varies from –65 to –90‰, but may even decrease to –128‰, the involvement of meteoric water in serpentinitization, is not ruled out.

#### 2.6. *Geodynamic Model*

Our model of the formation of the Karabash massif (Figure 5A) is based on the concept of the “blocky folding of the Earth’s crust” [14]. According to this model, the upper elastic crust is divided into huge blocks by the thrusts dipping toward each other as a result of applied horizontal force. The thrusts result in bends and deformation of blocks, thickening in the vertical plane, and shortening along the compression axis. The thickening and shortening of the upper crust generated a tectonic flow in the lower elastic crust and caused its thermodynamic destabilization.

The Moho boundary is the base of the tectonic flow of the lower crustal rocks. In areas of decompressed mantle, this tectonic flow descends downward. The lower crust rocks undergo high-temperature/high-pressure—metamorphism and dehydration and mix with the rocks of the decompressed upper mantle. The flow of the crust-mantle mixture, directed upward, penetrated the lower and then the upper crust. The upper crust rocks ascended and stretched to form mountain relief.

During the ascending process, the crust-mantle mixture trapped the portions of the non-metamorphosed lower crust and the sialic upper crust experienced decompressing, fracturing, and autometamorphism.

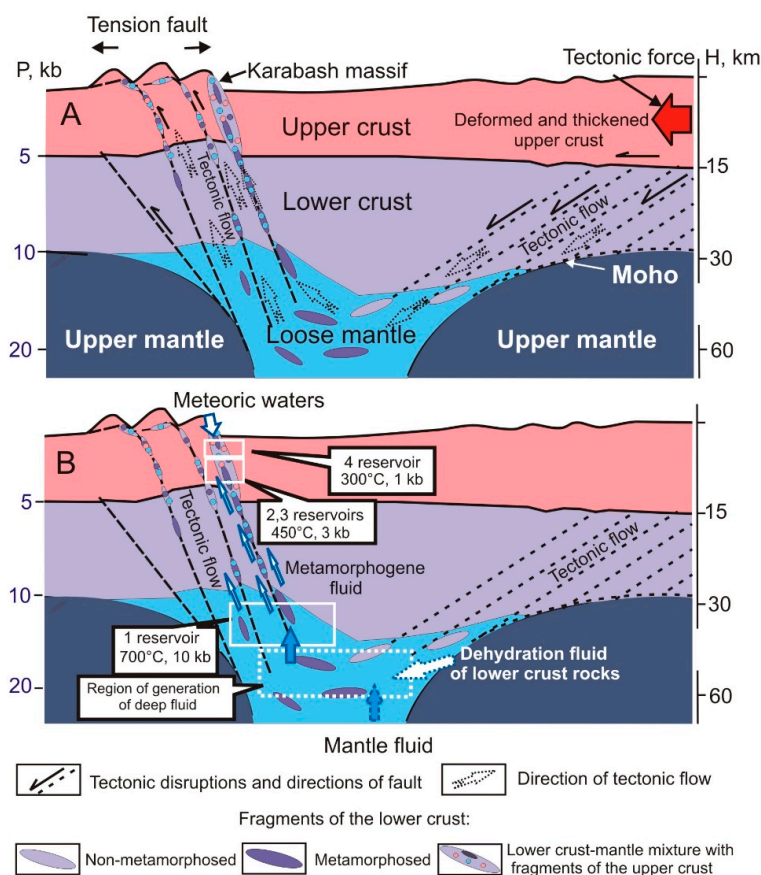


**Figure 5.** Model of the formation of the Karabash ultramafic massif and sources of ore-forming fluids. (A) Geodynamic model and (B) fluid model.

The application of the model of blocky folding of the Earth's crust to explain the tectonic setting of the Karabash massif is supported by the results of our research into minor structural forms, bodies of rotation, authors' interpretation of the seismic profile URSEIS-95, and deciphering space photographs [15]. Figure 5B shows the main sources of the fluid and the fluid components involved in the formation of the Karabash massif and the magnetite-chlorite-carbonate rocks therein. The main source of fluid was the juvenile water formed during the oxidation of the mantle hydrogen, as well the water separated during the dehydration and deserpentinization of the lower crust rocks. The fluid reacted with the rocks of the crust-mantle mixture, extracting various components. On the way to the surface, the tectonic flow was enriched in volcano-sedimentary rocks, including marine limestones, which also interacted with the fluid. Rapid decompression on the upper horizons was accompanied by the formation of large steeply dipping en-échelon extension cracks in which the deep fluid was percolated, filling the free space. Simultaneously, meteoric waters that arrived from the top along the extension cracks mixed with the deep fluid and reacted with serpentinites.

### 3. Methods

#### 3.1. Software and Thermodynamic Dataset for Modeling

Thermodynamic modeling was performed using the Selektor-C software that employs the Gibbs energy minimization method, including minerals, aqueous solution components, and gasses in given T, P-conditions [16,17]. We applied a similar approach for studying the gold-bearing

rodingites from the Zolotaya Gora deposit in the Karabash massif [6] and three stages of epithermal gold-silver mineralization of primary and placer gold deposits [18,19]. The main calculation procedures implementing the determination of thermodynamic parameters of compounds of a system at high T, P values were based on the following methods. The calculation of the thermodynamics for aqueous solution components was performed using the revised Helgeson-Kirkham-Flowers (HKF) equation [20]. The dependence of the thermodynamic characteristics of gases on pressure was calculated using the modified Benedict-Webb-Rubin equation of state [21]. In the high-pressure zone, a deviation from ideal gas mixture for real gases was calculated using the van der Waals equation [22] and data from Breedveld and Prausnitz [23]. Fugacity coefficients and molar gas volumes were calculated using the two- [23] and three-parameter equation of state [21].

Modeling was completed for the Na-K-Mg-Ca-Al-Si-Ti-Mn-Fe-Cu-Ag-Au-Hg-S-P-Cl-C-H-O system. The thermodynamic properties of various compounds were calculated using the Selektor-C database. The list of minerals, aqueous, and gaseous species considered in the model is provided in Tables S2 and S3 of the Supplementary Materials.

Thermodynamic constants for chlorites, ilmenites, pyroxenes, carbonates, olivines, and plagioclases, which are natural binary and ternary solid solutions, as well as solid solutions of quaternary system Ag-Au-Cu-Hg, were calculated considering the activity coefficients of end members for the accepted models of solid solutions [17,18]. Serpentine was introduced as an ideal solid solution consisting of antigorite and lizardite.

### 3.2. Initial Data for Thermodynamic Modeling

Our calculations were based on the reactive transport model involved in the Selektor-C software. Modeling was conducted at initial temperature (T) and pressure (P) characterizing the lower crust conditions: 700 °C and 10 kbar, respectively. The initial hydrothermal liquid consisted of (mole/kg H<sub>2</sub>O): NaCl = 1.5, CO<sub>2</sub> = 0.5, H<sub>2</sub> = 0.01, NaOH = 0.3, and H<sub>2</sub>S = 0.0001. The concentrations of NaCl were specified following the results of fluid inclusion studies [9] in magnetite-chlorite-carbonate rock. As the ore-forming system has minor sodium and sulfur contents, we added NaOH and H<sub>2</sub>S into the model solution. The following parameters were applied to the model solution: log  $f_{\text{O}_2}$  = −14.3, log  $f_{\text{S}_2}$  = −5.44, pH = 6.9. The amount of ore components in the model solution was used depending on the content of Cu, Ag, Au, and Hg in the ultramafic rocks from Southern Urals (Table 1).

**Table 1.** Average contents of gold (Au), silver (Ag), copper (Cu), and mercury (Hg) (ppm) in the massif of ultramafic rocks (Southern Urals, Russia).

	Ultramafic Rocks	Mafic Rocks
Au	0.01135 <sup>1</sup>	0.003925 <sup>1</sup>
Ag	0.14 <sup>2</sup>	0.11 <sup>2</sup>
Cu	6.15 <sup>1</sup>	31.7 <sup>1</sup>
Hg	0.02 <sup>2</sup>	0.07 <sup>2</sup>

<sup>1</sup> harzburgites from the Nuralinsky massif [24]; <sup>2</sup> upper part of continental crust [25].

The hydrothermal model evolved given its gradual flowing through the system of reservoirs up to final discharge at 300 °C and 1 kbar. The composition of meteoric waters diluting the deep fluid was specified as a nonmineralized rainwater: 1 kg H<sub>2</sub>O + 0.015 m CO<sub>2</sub> + 0.00032 m O<sub>2</sub> (25 °C, 1 bar), pH = 5.6, Eh = 0.89 [26].

The model included a 4-reservoir calculation scheme depicted in (Figure 6). In the first reservoir at 700 °C and 10 kbar, 1 kg of initial solution reacts with 100 g of rock consisting of 80% harzburgite + 20% gabbro, enriched in the components of these rocks. In the next reservoirs, a discharge zone was simulated as a result of the movement of fluid to upper horizons (T = 450 °C and P = 3 kbar) under different scenarios. In the second reservoir, we assumed interaction of the solution with serpentinite (100 g), and in the third reservoir, with limestone (5 g) and serpentinite (0.5 g) in the flow regime. In the fourth reservoir, mineral formation takes place in a closed system represented initially by serpentinite

(100 g), which was affected by the solution flowing from the second reservoir and meteoric waters that diluted the deep fluid and led to a decrease in T and P to 300 °C and 1 kbar, respectively.

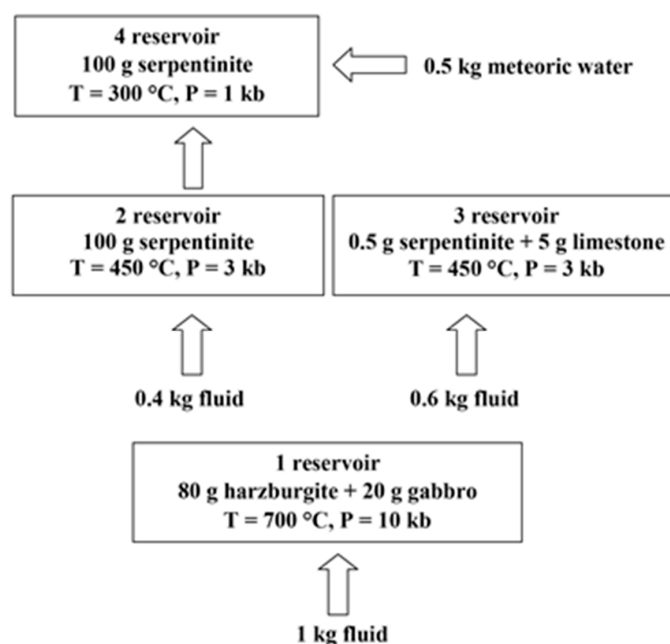


**Figure 6.** Scheme of the four-reservoir model.

We additionally constructed a version of a particular model in which we calculated the alterations in the composition of deep fluid from the first reservoir during ascent to the surface into the region of decreased temperatures and pressures (450–300 °C and 1–3 kbar).

The chemical compositions of rocks used in the model are provided in Table 2.

**Table 2.** Chemical compositions of rocks involved in the thermodynamic model.

	Gabbro (n = 7)	Harzburgite (n = 9)	Limestone	Serpentinite
SiO <sub>2</sub>	48.81	40.43	0.19	40.47
TiO <sub>2</sub>	0.37	0.04	-	0.04
Al <sub>2</sub> O <sub>3</sub>	14.65	1.52	0.18	1.44
Fe <sub>2</sub> O <sub>3</sub>	7.97	4.26	-	5.31
FeO	7.20	3.79	0.23	1.61
MnO	0.18	0.09	0.17	0.09
MgO	8.57	38.41	0.39	38.21
CaO	12.03	1.62	55.13	0.48
Na <sub>2</sub> O	2.75	0.11	-	0.12
K <sub>2</sub> O	0.44	0.03	-	0.03
P	0.09 *	0.035 *	-	0.013 **
S	-	-	-	0.75
CO <sub>2</sub>	-	-	43.75	0.46
LOI	1.96	6.77	-	10.59

Data for gabbro and harzburgite from Southern Urals (Talovsky massif) were borrowed from Gritsuk [27], for limestones at the contact of the Karabash massif, from Spiridonov and Pletnirov [4], for serpentinites from the Karabash massif, from Berzon [28]. Content of phosphorus: \* average content in mafic and ultramafic rocks of the upper mantle [25]; \*\* in serpentinites from the Karabash massif, our data (ICP-MS, n = 8).

#### 4. Results of Thermodynamic Modeling

##### 4.1. Fluid Composition and Forms of Transfer and Deposition of Au, Ag, Cu, and Hg

Sodium chloride-carbon dioxide ore-bearing fluid ( $\log f_{\text{O}_2} = -14.3$ ,  $\log f_{\text{S}_2} = -5.44$ ,  $\text{pH} = 6.9$ ) increased total dissolved solids (TDS) to 100 g/L during interaction with the rocks of the second and third reservoirs, and thereafter, being diluted with meteoric water, stabilized at  $\text{TDS} = 50$  g/L and  $\text{pH} = 7.4$ . Oxygen and sulfur fugacities depend mainly on temperature and gradually decreased in the range of  $\log f_{\text{O}_2} = -14/(-34)$  and  $\log f_{\text{S}_2} = -5/(-11)$  (Figure 7).

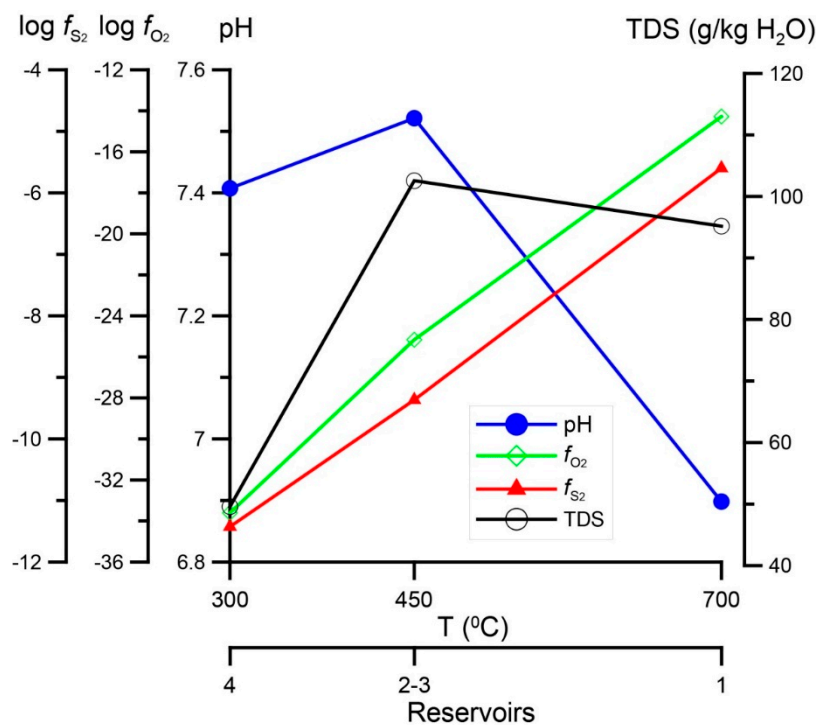


**Figure 7.** Variations in the values of pH, total dissolved solids (TDS), sulfur fugacity ( $\log f_{\text{S}_2}$ ), and oxygen fugacity ( $\log f_{\text{O}_2}$ ) in different reservoirs.

In the suggested model, the fluid extracted ore components from deeply-seated rocks, and the contents of metals in the fluid were taken to be close to those in ultramafic and mafic rocks of the upper crust and Nuralinsky massif in the Southern Urals (Table 1). To estimate the contents of deposited gold and to determine the composition of Au-Ag-Cu solid solutions, we performed calculations for four different metal contents in the fluid. The first variant included the contents of metals in the fluid equivalent to that in ultramafic rocks (U), the intermediate variants, in ultramafic and mafic rocks (U + M), and the last variant, in mafic rocks (M) (Figure 8a–h). These calculations show that the gold content in the rocks of the third reservoir increased with the supply of every new portion of solution from 0.7 to 20 g/t in the first variant and from 0.5 to 10 g/t in the last. Gold content in the fourth reservoir was high (about 10 g/t) only in the first case; in all other cases, the content of the deposited gold was less than 0.3 g/t.

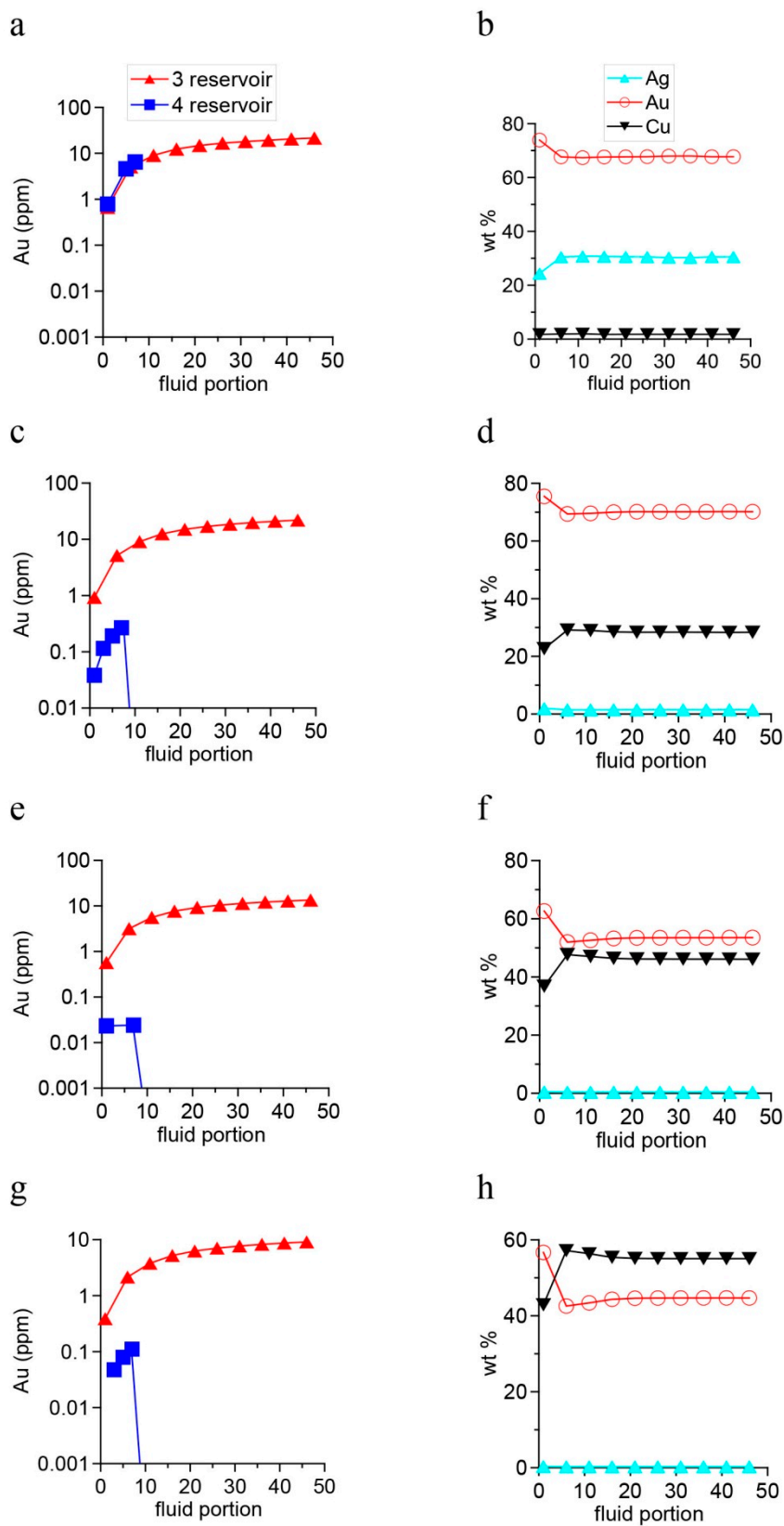


**Figure 8.** Distribution of gold in the model at the ratios of Au, Ag, Cu, and Hg in the fluid according to their average concentrations in ultramafic (U) and mafic (M) rocks (Table 1), specified in different proportions: (a,b) U, (c,d) 0.75 U and 0.25 M, (e,f) 0.25 U and 0.75 M, and (g,h) M. (a,c,e,g) Au in rock (third and fourth reservoirs); (b,d,f,h) components in Ag-Au-Cu solid solution (third reservoir).

The Au-Ag-Cu solid solutions in the third reservoir at  $T = 450\text{ }^{\circ}\text{C}$  were formed with the first portions of aqueous solution and their composition remained stable with further incoming solution. When the fluid source was in ultramafic rocks, the Cu-bearing Au-Ag solid solution with ratios (wt %) Au:Ag:Cu = 68:30:2 occurred. When the ratio of mafic rocks in the reservoir and the amount of ore components in the fluid increased, the solid phase contained silver-bearing Au-Cu solid solution with the amount of copper increasing from 28 to 55 wt % (Figure 8b,d,f,h). The sulfur fugacity ( $\log f_{\text{S}_2}$ ) was approx.  $-9.4$ . The comparison of different variants of the Au, Ag, and Cu ratios in the model solution at the preliminary stage became the basis for selecting ultramafic rocks with a minor fraction of mafic rocks as a source of ore components for further calculations.

Notably, the absence of degassing during the formation of magnetite-chlorite-carbonate rocks contributed to the fact that Au, Ag, Cu, and Hg do not preferably enter into a gas phase but accumulate in the hydrothermal solution, and when saturation is achieved, Au-Ag-Cu-Hg solid solution precipitates. Depending on the composition of hydrothermal solution and the evolution of its physicochemical parameters, the forms of metal complexes change during transfer and deposition of ore elements (Figure 9).

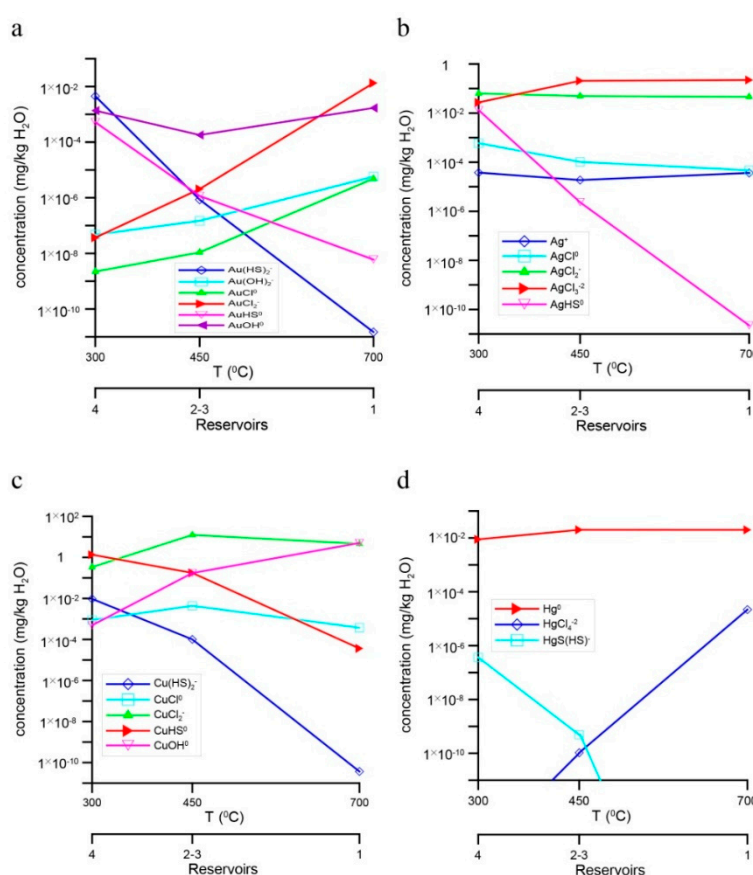


**Figure 9.** Content of different forms of metal complexes in ore-bearing solution containing average contents of ore components in ultramafic rocks: (a) Au, (b) Ag, (c) Cu, and (d) Hg.

In the suggested model, gold in the fluid (Figure 9a) in the first reservoir (700 °C) is mainly represented by chloride complex AuCl<sub>2</sub><sup>-</sup> [29]. Thereafter, when the fluid was transported to the next reservoirs and the temperature decreased, its amount decreased significantly: at 450 °C, the main gold-bearing complex is hydroxocomplex AuOH<sup>0</sup> in the presence of small amounts of Au(HS)<sub>2</sub><sup>-</sup> and AuHS<sup>0</sup> [30], and at 300 °C, the role of gold sulfide complexes increased drastically [29].

NaCl-rich fluid determines the predominance of chloride complexes of Ag and Cu in the 1.–3. reservoirs (Figure 9b,c). In contrast to silver, the copper hydrocomplex CuOH<sup>0</sup> is also present in the

fluid. Mercury, opposed to Au, Ag, and Cu, is primarily present in the solution as  $Hg^0$ , whereas chloride and sulfide complexes are minor (Figure 9d).

#### 4.2. Specific Features of Mineral Composition of Rocks in Different Reservoirs of the Model

Mineral compositions of rocks in different reservoirs of the model are presented in Figure 10. The first reservoir corresponds to the lower crust rocks and has a stable set of minerals, dominated by olivine (to 70 wt %) accompanied by smaller amounts of garnet, magnetite, and chlorite (Figure 10a). In the second reservoir, imitating the deep fluid infiltration through serpentinites, magnetite (less than 10%) and carbonate (less than 3%) appear as minerals in equilibrium with serpentine. The other stages of the process are marked by the occurrence of pyroxene, talc, and tremolite (Figure 10b). Through the third reservoir, the fluid passed in a flow mode, interacting with a minor amount of host rocks (serpentinites), which can be interpreted as precipitation of minerals from the fluid in an open crack system. Within the third reservoir, a mixture of carbonate (to 70 wt %), magnetite (to 30 wt %) and a small amount of chlorite (to 5 wt %) was within open cavities and cracks. Pyroxene formed from the first portions of solution became unstable (Figure 10c). The composition of carbonate solid solution was dominated by calcite. In the fourth reservoir, mineral formation occurred in a closed system in which serpentinite was replaced by chloritilite, a rock composed of chlorite (to 90%) and small amounts of talc and carbonate (Figure 10d). Ilmenite and hydroxyapatite were accessory minerals in all reservoirs. In addition, chalcocopyrite up to 0.2 wt % was formed in the fourth reservoir. Gold was deposited at all stages of the rock-water interaction during the formation of magnetite-chlorite-carbonate rocks (third reservoir) and at the initial stages in the fourth reservoir, when the transformation of serpentinites initialized (Figure 10c,d).

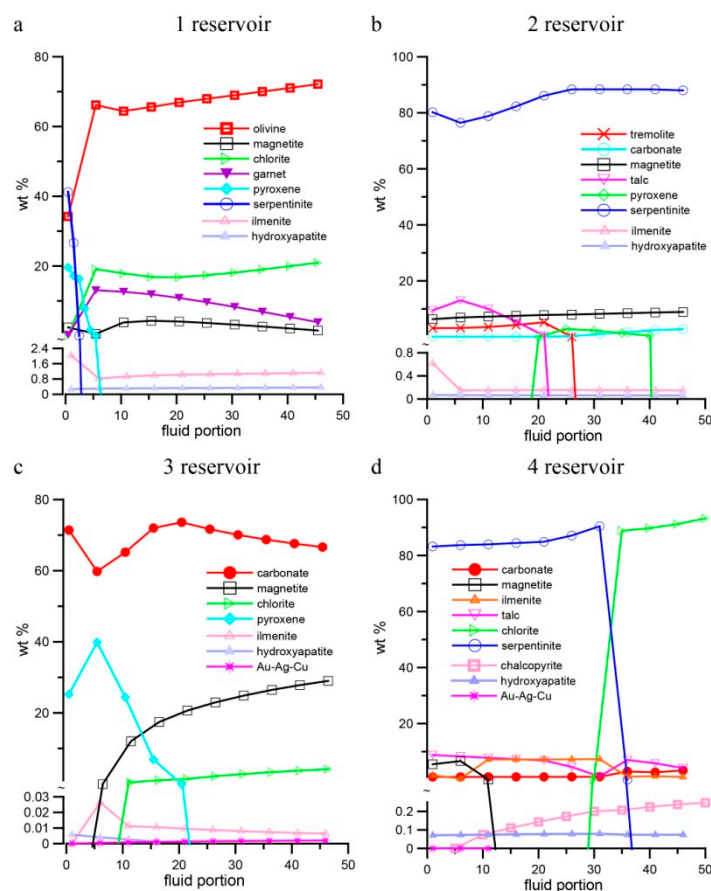


**Figure 10.** (a–d) Changes in the mineral composition of model reservoirs 1–4, respectively, as the amount of incoming fluid increases.

### 4.3. Uplift of Deep-Seated Rocks under Low T,P-Conditions

To analyze the changes in the mineral composition during the ascent of deep-seated rocks into the region of lower temperatures and pressures, we considered a particular model in which mineral associations were calculated in the range of  $T = 300\text{--}700\text{ }^{\circ}\text{C}$  and  $P = 1\text{--}10\text{ kbar}$  based on the chemical composition of chlorite-olivine rocks (Figure 11).

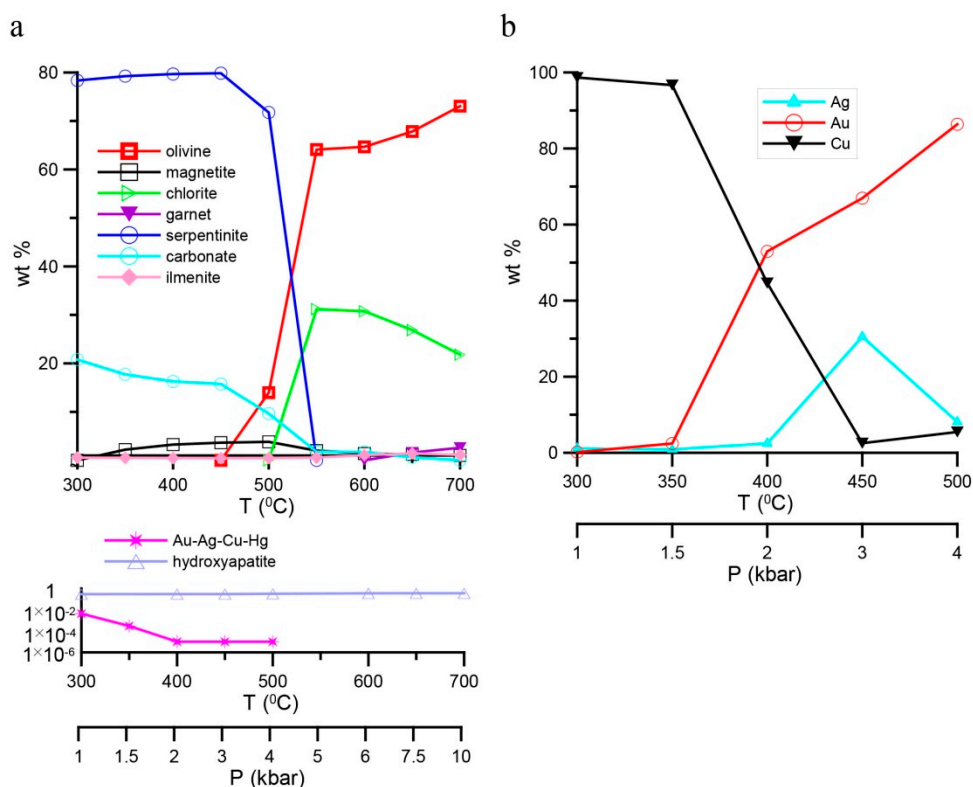


**Figure 11.** Mineral composition of (a) rocks and (b) Au-Ag-Cu solid solutions in changing pressure (P) and temperature (T) conditions.

When  $T = 450\text{--}300\text{ }^{\circ}\text{C}$  and  $P = 3\text{--}1\text{ kbar}$ , the olivine-rich rock was replaced by the carbonate-serpentine rocks with a mineral composition similar to serpentinite from the second reservoir of the basic model. It contained up to 15–20 wt % carbonate (mainly of magnesian composition), a small amount (up to 5 wt %) magnetite and less than 1 wt % ilmenite, apatite, and Au-Ag-Cu in solid solution (Figure 11a).

The Au-Ag-Cu composition of solid solution varied from copper gold (8% Ag + 87% Au + 5% Cu) at 500 °C to copper-bearing electrum (30.5% Ag + 67% Au + 2.5% Cu) at 450 °C, which, after a further decrease in temperature to 300 °C, was replaced by native copper with minor admixture of silver and gold (98.8% Cu + 1% Ag + 0.2% Au) (Figure 11b).

## 5. Discussion

### 5.1. Similarity of Natural and Model Composition of Rocks and Gold Mineralization

Our calculations provide good similarity of the modeled and natural minerals compositions of altered rocks from the Karabash massif. Although garnet-chlorite-olivine rocks corresponding to the mineral composition of the first reservoir have not been found near the present-day erosion level, they are suggested to occur at a considerably deeper level or, most likely, their mineral composition was altered during the movement of rocks and fluids to the region of lower temperatures and pressures.

The calculated particular model (Figure 11) shows the possibility of transformation of essentially olivine-rich rocks to serpentinite with a small amount of carbonate and magnetite. Similar serpentinites are a significant part of the Karabash massif. They commonly contain native copper, whose origin is confirmed by the thermodynamic calculations at 300 °C. Model calculations at 450 °C corroborate the formation of copper-bearing Au-Ag solid solution and copper sulfides in serpentinites.

The gold-bearing rocks composed of magnetite, chlorite, and carbonate formed in the third reservoir modeling the decompression in open cracks. The P,T-parameters accepted for this reservoir were similar to the formation conditions of magnetite-chlorite-carbonate rocks (480–280 °C, 2–3 kbar). The quantitative ratios of the main minerals (magnetite, chlorite, and carbonate) in the model reservoir correspond to their variations in natural parageneses. Good correlation of model and natural parageneses was observed in the set of accessory minerals of rocks. In both cases, they are represented by ilmenite, apatite, chalcopyrite, and Au-Ag-Cu solid solutions.

The calculated composition of Au-Ag-Cu solid solutions in the third reservoir is similar to the composition of native gold in magnetite-chlorite-carbonate rocks. The model solid solution differs from copper gold of the Karabash ultramafic massif only in terms of a slightly higher silver content. Moreover, the calculation results of various metal ratios in solution showed that the deep-seated rocks of ultramafic composition with a minor fraction of mafic rocks (0.75 U and 0.25 M) (Figure 8c,d) were the most probable source of these metals. An increase in the fraction of mafic rocks in the model led to the formation of Au-Cu solid solutions that were not observed in magnetite-chlorite rocks.

Association of chloritoid and magnetite-chlorite-carbonate rock is reflected in one of the variants of the model calculations—on cooling of serpentinites of the second reservoir to 300 °C and dilution of the equilibrium fluid by meteoric waters approximately in equal ratios. As this association of rocks in the Karabash massif created submeridionally stretching schist zones, we suggest that meteoric waters infiltrated from the top along tectonic faults into serpentinites toward the deep-seated fluid ascending through the same faults.

The presence of gold and REE in the deep-seated rock source was the main factor influencing the high concentrations of these elements in the magnetite-chlorite-carbonate rocks. We analyzed the model devoid of Y, Zr, REE, U, and Th mineralization due to the complex mineral composition of altered ultramafic rocks from the Karabash massif. This is one of the prospective tasks that will be solved to reveal the simultaneous formation conditions of gold and Y, Zr, REE, U, Th mineralization.

## 5.2. Scales of Gold Mineralization in the Karabash Massif and the Variations in the Compositions of Gold Minerals

Gold mineralization, including various intermetallides and solid solutions of the Au-Ag-Cu-(Hg) system, occurred in virtually all types of altered ultramafic rocks in the Karabash massif. Our previous physicochemical models of formation of gold-bearing rodingites [6] and magnetite-chlorite-carbonate rocks, serpentinites, and chloritoidites, presented in this work, support the variety of minerals forms and different concentrations of Au, Ag, and Cu (Hg) in the rocks of the massif. The maximum gold concentration was determined to be in the rodingites. The gold content in the Zolotaya Gora deposit reaches several hundred ppm, averaging 5 ppm. These rocks are also characterized by the greatest variety of mineral forms of gold—Au-Cu intermetallides (tetra-auricupride AuCu, auricupride AuCu<sub>3</sub>, and Au<sub>3</sub>Cu) and solid solutions of the Au-Ag-Hg system.

Gold concentrations in the third and fourth reservoirs in the model calculated in this work (0.3–30 ppm) correspond to the concentration levels in the magnetite-chlorite-carbonate rocks and chloritoidites. In magnetite-chlorite-carbonate rocks, the amount of copper-bearing Au-Ag solid solution may be high, but the small sizes of these rocks do not allow them to be considered objects for mining.

In addition to rodingites and magnetite-chlorite-carbonate rocks, other altered rocks, mainly listvenites and quartz-riebeckite metasomatites, have also been found in the Karabash massif. These rocks either do not contain or are poor in gold. However, in the Southern Urals within the zone of the Main Ural Fault, many auriferous ore deposits have been found in listvenites (Nailinskoe,

Tyelginskoe, Altyn-Tashskoe, and Mechnikovskoe, etc.) [31]. The chemical composition of the native gold in these deposits is similar to the most widespread Au-Ag solid solution containing no less than 1 wt % copper.

Our calculations show that the copper-bearing Au-Ag solid solution could have formed via the participation of the ore fluid during the serpentinization of deep-seated olivine rocks pumped by the tectonic flow to a higher hypsometric level. Data on gold content in serpentinites from the Karabash massif are unknown. However, in the other Ural massifs, antigorite serpentinites confined to the fault zones bear gold mineralization and are the source of gold in the placers [32].

## 6. Conclusions and Perspectives

We developed a physicochemical model of the formation of ophiolite serpentinites of specific rocks that host gold mineralization with a very low sulfide content. Using thermodynamic calculations, we obtained mineral associations of gold-bearing (magnetite-chlorite-carbonate) and weakly gold-bearing rocks (serpentinites and chloritolites) similar to those occurring in the Karabash massif in the Southern Urals. These rocks formed with the participation of meteoric waters and the deep-seated fluid that changed its composition during the tectonic movement of the crustal-mantle mixture to the surface. The copper gold can precipitate during serpentinization of deep-seated olivine-rich rocks uplifted by the tectonic flow to a higher hypsometric level.

The model supports the involvement of sodium chloride-carbon dioxide fluids extracting ore components (Au, Ag, and Cu) from deep-seated ultramafic rocks with a minor admixture of mafic rocks. The developed model of tectonic squeezing of the deep-seated fluid, crust and mantle rocks allows the prediction of the copper gold ore occurrences in ultramafic ore massifs. At the same time, a more complex model should be developed that also involves Y, Zr, REE, U, and Th mineralization.

**Supplementary Materials:** The following are available online at: <http://www.mdpi.com/2075-163X/8/7/306/s1>, Table S1: Trace-element composition of rocks (ppm), Table S2: Components of aqueous solution and gases considered in thermodynamic models, Table S3: Solid phases components used in thermodynamic models.

**Author Contributions:** V.M., K.C. and C.P. made substantial contributions to the conception of the work and interpretation of data and wrote the paper. K.C. performed the thermodynamic calculations. A.K. revised the geological section. D.V. studied the mineral associations in the rocks and analyzed the compositions of minerals.

**Funding:** This work was supported by the Russian Foundation for Basic Research (grant 16-05-00407a) and state assignment projects (Nos. 0330-2016-0001, 0350-2016-0033 and 0393-2016-0024).

**Acknowledgments:** We thank the reviewers for important comments and constructive suggestions which helped us to significantly improve the quality of the manuscript. Special thanks go to the reviewers for correcting the English language of the manuscript. We thank Kiselev, V.D., Garaeva, A.A., Velivetskaya, T.A. and Shanina, S.N. for the analytical data.

**Conflicts of Interest:** The authors declare no conflict of interest.

## References

1. Puchkov, V.N. General features relating to the occurrence of mineral deposits in the Urals: What, where, when and why. *Ore Geol. Rev.* **2017**, *85*, 4–29. [CrossRef]
2. Snachyov, A.V.; Kuznetsov, N.S.; Snachyov, V.I. The Chernoe ozero gold occurrence in carbonaceous deposits of the ophiolite association: The first object of such a type in the Southern Urals. *Dokl. Earth Sci.* **2011**, *439*, 906–908. [CrossRef]
3. Novgorodova, M.I.; Tsepin, A.I.; Kudrevich, I.M.; Vyal'sov, L.N. New data on crystal chemistry and properties of natural intermetallic compounds in the copper-gold system. *Zap. Vses. Miner. Obsch.* **1977**, *106*, 540–552. (In Russian)
4. Spiridonov, E.M.; Pletniyov, P.A. *Zolotaya Gora Deposit of Cupriferous Gold (About "Golden-Rodingite" Formation)*; Scientific World: Moscow, Russia, 2002; p. 220. ISBN 5-89176-169-6. (In Russian)
5. Murzin, V.V.; Varlamov, D.A.; Ronkin, Y.L.; Shanina, S.N. Origin of Au-bearing Rodingite in the Karabash Massif of Alpine-Type Ultramafic Rocks in the Southern Urals. *Geol. Ore Depos.* **2013**, *55*, 278–297. [CrossRef]

6. Murzin, V.V.; Chudnenko, K.V.; Palyanova, G.A.; Varlamov, D.A.; Naumov, E.A.; Pirajno, F. Physicochemical model of formation of Cu-Ag-Au-Hg solid solutions and intermetallic alloys in the rodingites of the Zolotaya Gora gold deposit (Urals, Russia). *Ore Geol. Rev.* **2018**, *93*, 81–97. [[CrossRef](#)]
7. Murzin, V.V.; Popov, V.A.; Erokhin, Y.V.; Rakhov, E.V. Mineralogic and Geochemical Features of Gold-Rare-Metal-Rare-Earth Mineralization of Chlorite-Carbonate Rocks from the KARABASH Massif of Ultrabasic Rocks (Southern Urals). In *Ural'skii Mineralogicheskii Sbornik*; IMin UrO, RAS: Miass, Russia, 2005; Volume 13, pp. 123–145. (In Russian)
8. Murzin, V.V.; Varlamov, D.A.; Palyanova, G.A. Conditions of formation of gold-bearing magnetite–chlorite–carbonate rocks of the Karabash ultrabasic massif (South Urals). *Russ. Geol. Geophys.* **2017**, *58*, 803–814. [[CrossRef](#)]
9. Murzin, V.V.; Shanina, S.N. Physic-chemical conditions of gold-bearing magnetite-chlorite-carbonate rocks' formation of the Karabash ultramafic massif (the Southern Urals). *Litosphera* **2017**, *17*, 110–117. [[CrossRef](#)]
10. Lozhechkin, M.P. *The Karabash Deposit of Cupriferous Gold*; Trudy UFAN SSSR: Sverdlovsk, Russia, 1935; pp. 35–44. (In Russian)
11. Borisenko, A.S. Study of the salt composition of solutions in gasliquid inclusions in minerals by the cryometric method. *Sov. Geol. Geophys.* **1977**, *18*, 11–19.
12. Bodnar, R.J.; Vityk, M.O. Interpretation of microthermometric data for H<sub>2</sub>O-NaCl fluid inclusions. In *Fluid Inclusions in Minerals: Methods and Applications*, 2nd ed.; De Vivo, B., Frezzotti, M.L., Eds.; Virginia Tech: Blacksburg, VA, USA, 1994; pp. 117–130.
13. Roedder, E. Fluid inclusions. *Rev. Mineral.* **1984**, *12*, 1–644.
14. Kisin, A.Y.; Koroteev, V.A. *Block Folding and Oreogenesis*; IGG UrB RAS: Ekaterinburg, Russia, 2017; p. 349. (In Russian)
15. Kissin, Y.; Murzin, V.V.; Pritchkin, M.E. Tectonic position of the gold mineralization of the Karabash Mountain (Southern Urals): Examination of small structural forms. *Litosphera* **2016**, *16*, 79–91. (In Russian)
16. Karpov, I.K.; Chudnenko, K.V.; Kulik, D.A. Modeling chemical mass-transfer in geochemical processes: Thermodynamic relations, conditions of equilibria and numerical algorithms. *Am. J. Sci.* **1997**, *297*, 767–806. [[CrossRef](#)]
17. Chudnenko, K.V. *Thermodynamic Modeling in Geochemistry: Theory, Algorithms, Software, Applications*; Academic Publishing House Geo: Novosibirsk, Russia, 2010; 287p, ISBN 978-5-904682-18-7. (In Russian)
18. Chudnenko, K.V.; Palyanova, G.A. Thermodynamic modeling of native formation Cu-Ag-Au-Hg solid solutions. *Appl. Geochem.* **2016**, *66*, 88–100. [[CrossRef](#)]
19. Zhuravkova, T.V.; Palyanova, G.A.; Chudnenko, K.V.; Kravtsova, R.G.; Prokopyev, I.R.; Makshakov, A.S.; Borisenko, A.S. Physicochemical models of formation of gold–silver ore mineralization at the Rogovik deposit (Northeastern Russia). *Ore Geol. Rev.* **2017**, *91*, 1–20. [[CrossRef](#)]
20. Tanger, J.C.; Helgeson, H.C. Calculation of the thermodynamic and transport properties of aqueous species at high pressures and temperatures: Revised equations of state for standard partial molal properties of ions and electrolytes. *Am. J. Sci.* **1988**, *288*, 19–98. [[CrossRef](#)]
21. Lee, B.I.; Kesler, M.G. Generalized thermodynamic correlation based on three parameter corresponding states. *AIChE J.* **1975**, *21*, 510–527. [[CrossRef](#)]
22. Walas, S.M. *Phase Equilibria in Chemical Engineering*; Butterworth Publishers: Boston, MA, USA, 1985; 671p, ISBN 978-0-409-95162-2.
23. Breedveld, G.J.F.; Prausnitz, J.M. Thermodynamic properties of supercritical fluids and their mixtures at very high pressure. *AIChE J.* **1973**, *19*, 783–796. [[CrossRef](#)]
24. Garuti, G.; Fershtater, G.B.; Bea, F.; Montero, P.; Pushkarev, E.V.; Zaccarini, F. Platinum Group Elements As a Petrological Indicators in Mafic-Ultramafic Complexes of the Central and Southern Urals: Preliminary Results. *Tectonophysics* **1997**, *276*, 181–194. [[CrossRef](#)]
25. Grigoriev, N.A. *Chemical Element Distribution in the Upper Continental Crust*; UB RAS: Ekaterinburg, Russia, 2009; p. 382. (In Russian)
26. Karpov, I.K.; Chudnenko, K.V.; Kravtsova, R.G.; Bychinskiy, V.A. Simulation modeling of physical and chemical processes of dissolution, transport and deposition of gold in epithermal gold-silver deposits of the North-East Russia. *Russ. Geol. Geophys.* **2001**, *3*, 393–408.
27. Gritsuk, N.A. Petrogeochemical Features and Pre Potential of the Talov Massif of Gabbro-Hyperbasic Rocks. Ph.D. Thesis, Moscow State University, Russia, 2003; p. 148. (In Russian)

28. Berzon, R.O. *Gold Resource Potential of Ultramafics*; VIEMS: Moscow, Russia, 1983; p. 47. (In Russian)
29. Zotov, A.; Kuzmin, N.; Reukov, V.; Tagirov, B. Stability of  $\text{AuCl}_2^-$  from 25 to 1000 °C at pressures to 5000 bar, and consequences for hydrothermal gold mobilization. *Minerals* **2018**, *8*, 286. [[CrossRef](#)]
30. Seward, T.M.; Williams-Jones, A.E.; Migdisov, A.A. The chemistry of metal transport and deposition by ore-forming hydrothermal fluids. In *Treatise on Geochemistry*, 2nd ed.; Turekian, K., Holland, H., Eds.; Elsevier: Amsterdam, The Netherlands, 2014; Volume 13, pp. 29–57.
31. Belogub, E.V.; Melekestseva, I.Y.; Novoselov, K.A.; Zabolotina, M.V.; Tret'yakov, G.A.; Zaykov, V.V.; Yuminov, A.M. Listvenite-related gold deposits of the South Urals (Russia): A review. *Ore Geol. Rev.* **2017**, *85*, 247–270. [[CrossRef](#)]
32. Murzin, V.V.; Varlamov, D.A.; Shanina, S.N. New Data on the Gold–Antigorite Association of the Urals. *Dokl. Earth Sci.* **2007**, *417A*, 1436–1439. [[CrossRef](#)]



© 2018 by the authors. Licensee MDPI, Basel, Switzerland. This article is an open access article distributed under the terms and conditions of the Creative Commons Attribution (CC BY) license (<http://creativecommons.org/licenses/by/4.0/>).